LA-UR 95-2015

CONF-9509100--22

Los Alamos National Laboratory is operated by the University of California for the United States Department of Energy under contract W-7405-ENG-36.

TITLE: MCNP PERTURBATION TECHNIQUE FOR CRITICALITY ANALYSIS

AUTHOR(S): G.W. McKinney
J.L. Iverson

SUBMITTED TO: ICNC Meeting, Albuquerque, NM, Sept. 17-21, 1995

DISCLAIMER

Los Alamos Los Alamos National Laboratory
Los Alamos, New Mexico 87545

FORM NO. 836 R4
ST NO 2629 5/81

DISTRIBUTION OF THIS DOCUMENT IS UNLIMITED GH

MASTER

MCNP Perturbation Technique For Criticality Analysis

G.W. McKinney and J.L. Iverson
Los Alamos National Laboratory
Los Alamos, NM 87545
(505)665-8367
(505)665-5538 Fax
gwm@lnal.gov

ABSTRACT

The differential operator perturbation technique has been incorporated into the Monte Carlo N-Particle transport code MCNP™ [1] and will become a standard feature of future releases. This feature includes first and/or second order terms of the Taylor Series expansion for response perturbations related to cross-section data (i.e., density, composition, etc.). Criticality analyses can benefit from this technique in that predicted changes in the track-length tally estimator of K_{eff} may be obtained for multiple perturbations in a single run. A key advantage of this method is that a precise estimate of a small change in response (i.e., < 1%) is easily obtained. This technique can also offer acceptable accuracy, to within a few percent, for up to 20-30% changes in a response.

INTRODUCTION

As given by the Taylor Series expansion, the evaluation of response sensitivities to cross-section data involves finding the ratio of the change in response to the infinitesimal change in the data. In deterministic methods, this ratio is approximated by performing two calculations, one with the original data and one with the perturbed data. This approach is useful even when the magnitude of the perturbation becomes very small. In Monte Carlo methods, however, this approach fails as the magnitude of the perturbation becomes small due to the uncertainty associated with the response. For this reason, the differential operator technique was developed.

The differential operator perturbation technique as applied to the Monte Carlo method was introduced in the early 1970's [2]. Nearly a decade after its introduction, this technique was applied to perturbations in cross-section data by Hall [3,4] and later Rief [5]. A rudimentary implementation into the Monte Carlo transport code MCNP followed shortly thereafter [6]. With an enhancement of the user interface and the addition of second order effects, this implementation has evolved into a standard feature of future MCNP releases.

In the following sections, the theory of this technique is reviewed, an overview of the MCNP user interface is given, and results for two criticality applications are presented.

DIFFERENTIAL OPERATOR TECHNIQUE

Derivation Of The Operator

MCNP is a trademark of the Regents of the University of California, Los Alamos National Laboratory.

In the differential operator approach, a change in the Monte Carlo response c, due to changes in the related data set (represented by the parameter v) is given by a Taylor series expansion

$$\Delta c = \frac{dc}{dv}\cdot\Delta v + \frac{1}{2!}\cdot\frac{d^2c}{dv^2}\cdot\Delta v^2 + \ldots + \frac{1}{n!}\cdot\frac{d^nc}{dv^n}\cdot\Delta v^n + \ldots$$

where the n^{th} order coefficient, u_n, is given by

$$u_n = \frac{1}{n!}\cdot\frac{d^nc}{dv^n}$$

which can be written as

$$u_n = \frac{1}{n!}\sum_{b\in B}\sum_{h\in H} x_b^n(h)\left(\frac{\partial^n c}{\partial x_b^n(h)}\right) \qquad (1)$$

for the data set

$$\{x_b(h) = K_b(h)\cdot e^v;\quad b\in B, h\in H\}$$

where $K_b(h)$ is some constant, B represents a set of macroscopic cross-sections, and H represents a set of energies or an energy interval. For a track based response estimator

$$c = \sum_j t_j q_j$$

where t_j is the response estimator and q_j is the probability of path segment j (path segment j is comprised of segment j-1 plus the current track). Equation (1) becomes

$$u_n = \frac{1}{n!}\sum_j \gamma_{nj} t_j q_j \qquad (2)$$

where

$$\gamma_{nj} \equiv \sum_{b\in B}\sum_{h\in H} x_b^n(h)\left(\frac{\partial^n}{\partial x_b^n(h)}(t_j q_j)\right)\left(\frac{1}{t_j q_j}\right)$$

With some manipulations presented in Reference [6], the path segment estimator of equation (2) can be converted to a particle history estimator

$$u_n = \sum_i V_{ni} p_i$$

where V_{ni} is the n^{th} order coefficient estimator for the i^{th} history and is given by

$$V_{ni} \equiv \frac{1}{n!}\sum_{j'} \gamma_{nj'} t_{j'} \qquad (3)$$

Note this sum involves only those path segments j' in particle history i. Equation (3) shows how the history estimator for the n^{th} order coefficient can be computed from the track (or path segment) based operator $\gamma_{nj'}$. The Monte Carlo expected value of u_n becomes

$$\langle u_n\rangle = \frac{1}{N}\sum_i V_{ni}$$

$$= \frac{1}{Nn!}\sum_i\left(\sum_{j'}\gamma_{nj'}t_{j'}\right) \qquad (4)$$

for a sample of N particle histories. Computing the n^{th} order differential operator $\gamma_{nj'}$ follows.

First Order

For a first order perturbation, the differential operator becomes

$$\gamma_{1j'} = \sum_{b\in B}\sum_{h\in H} x_b(h)\left(\frac{1}{q_{j'}}\right)\left(\frac{\partial q_{j'}}{\partial x_b(h)}\right)$$

assuming the response estimator t_j is not a function of $x_b(h)$. The path segment probability can be written as the product of track probabilities

$$q_j = \prod_{k=0}^{m} r_k$$

where r_k is the probability of track k and segment j contains m+1 tracks. In terms

of tracks, the operator becomes

$$\gamma_{1j'} = \sum_{k=0}^{m}\left[\sum_{b\in B}\sum_{h\in H} x_b(h)\left(\frac{1}{r_k}\right)\left(\frac{\partial r_k}{\partial x_b(h)}\right)\right]$$

or

$$\gamma_{1j'} = \sum_{k=0}^{m}\beta_{j'k} \qquad (5)$$

where

$$\beta_{j'k} \equiv \sum_{b\in B}\sum_{h\in H} x_b(h)\left(\frac{1}{r_k}\right)\left(\frac{\partial r_k}{\partial x_b(h)}\right) \qquad (6)$$

Defining track probabilities, r_k, in terms of Monte Carlo transport parameters is the final step of this derivation. If the k^{th} track starts with a neutron undergoing reaction type "a" at energy E′ and is scattered from angle θ′ to angle θ and E, continues for a length λ_k, and collides, then

$$r_k = \left(\frac{x_a(E')}{x_T(E')}\right)P_a(E'\to E;\theta'\to\theta)\,dEd\theta \cdot (e^{-x_T(E)\lambda_k})\,x_T(E)\,d\lambda \qquad (7)$$

where $x_a(E')$ is the macroscopic reaction cross-section at energy E′, $x_T(E')$ is the total cross-section at energy E′, and $P_a(E'\text{->}E;\theta'\text{->}\theta)dEd\theta$ is the probability distribution function in phase space of the emerging neutron. Equation (5) becomes

$$\beta_{j'k} = \sum_{b\in B}\sum_{h\in H}\left(\delta_{hE}\delta_{ba} - \frac{\delta_{hE}x_b(E)}{x_T(E)} - \delta_{hE}x_b(E)\lambda_k + \frac{\delta_{hE}x_b(E)}{x_T(E)}\right) \qquad (8)$$

where δ_{hE} and δ_{ba} are unity if h=E and b=a, otherwise they vanish. Similarly for other types of tracks (i.e., collision to boundary, boundary to collision, and boundary to boundary), leading to one or more of these four terms. Finally, combining equations (4) and (5) gives

$$\langle u_1\rangle = \frac{1}{N}\sum_i\left[\sum_j\left(\sum_{k=0}^{m}\beta_{j'k}\right)t_j\right]$$

where $\beta_{j'k}$ is calculated from one or more terms of equation (8) for track k.

Second Order

For a second order perturbation, the differential operator becomes

$$\gamma_{2j'} = \sum_{b\in B}\sum_{h\in H} x_b^2(h)\left(\frac{1}{q_{j'}}\right)\left(\frac{\partial^2 q_{j'}}{\partial x_b^2(h)}\right)$$

again assuming the response estimator t_j is not a function of $x_b(h)$. Omitting steps presented in Reference [7], the second order operator becomes

$$\gamma_{2j'} = \sum_{k=0}^{m}(\alpha_{j'k}-\beta_{j'k}^2) + \left(\sum_{k=0}^{m}\beta_{j'k}\right)^2$$

where

$$\alpha_{j'k} \equiv \sum_{b\in B}\sum_{h\in H} x_b^2(h)\left(\frac{1}{r_k}\right)\left(\frac{\partial^2 r_k}{\partial x_b^2(h)}\right)$$

It is evident that $\gamma_{2j'}$ requires little additional effort to $\gamma_{1j'}$, namely the computation of $\alpha_{j'k}$. If r_k is given by equation (7), then $\alpha_{j'k}$ becomes

$$\alpha_{j'k} = \sum_{b\in B}\sum_{h\in H}\left(\frac{2\delta_{hE}x_b^2(E)}{x_T^2(E)} - \frac{2\delta_{hE}\delta_{ba}x_b(E)}{x_T(E)} + \delta_{hE}x_b^2(E)\lambda_k^2 - \frac{2\delta_{hE}x_b^2(E)\lambda_k}{x_T(E)}\right)$$

Once again, for other types of tracks one or more of these four terms is required. The second order coefficient estimator, given by equation (4), becomes

$$\langle u_2\rangle = \frac{1}{2N}\sum_i\left[\sum_j\left(\sum_{k=0}^{m}(\alpha_{j'k}-\beta_{j'k}^2) + \left(\sum_{k=0}^{m}\beta_{j'k}\right)^2\right)t_j\right]$$

MCNP USER INTERFACE

General Description

The PERT card allows the user to make perturbations in cell material density, composition, or cross-section data. Using the differential operator technique, the perturbation estimates are made without actually changing the input material specifications. Multiple perturbations can be applied in the same run, each specified by a separate PERT card. There is no limit to the number of perturbations, since dynamic memory is used for perturbation storage. The entire tally output is repeated for each perturbation, giving the estimated differential change in the tally or alternately this change added to the unperturbed tally (see the METHOD keyword). Perturbations to the K_{eff} estimator can be made by use of a track-length tally estimate of K_{eff}. The CELL keyword and either the MAT or RHO keyword are required.

PERT Card Keywords

CELL - The entry(s) following this keyword indicate which cells are perturbed.

MAT - The entry following this keyword specifies the perturbation material number, which must have a corresponding M card. Composition changes can only be made through the use of this keyword.

RHO - Specifies the perturbed density of the cells listed after the CELL keyword.

METHOD - This keyword specifies the number of terms to include in the perturbation estimate.

1 - include 1st and 2nd order (default)

2 - include only 1st order

3 - include only 2nd order

A positive entry produces perturbation tallies which give the estimated **differential** change in the unperturbed tally (default). A negative entry generates perturbation tallies such that this change is **added** to the unperturbed tally. The ability to produce first and second order terms separately enables the user to determine the significance of including the second-order estimator for subsequent runs.

ERG - The two entries following this keyword specify an energy range in which the perturbation is applied. The default range includes all energies.

RXN - The entries following this keyword must be ENDF/B reaction types that identify one or more cross-sections to perturb. This keyword allows the user to perturb a specific cross-section of a single nuclide in a material, as well as to perturb a set of cross-sections for all nuclides in a material. The default is the total cross-section.

APPLICATION RESULTS

Ten test problems were developed to validate the accuracy of the differential operator technique in MCNP. These problems were taken from the MCNP 25 problem test set and included eight fixed-source problems (neutron, photon, and coupled), as well as two criticality problems [7]. Perturbation results for the criticality problems follow.

First Problem

This problem is INP09 from the MCNP test set and is comprised of a cubic shaped piece of ^{235}U (see Figure 1). The cube is approximately 10 cm on each side and is centered at the origin. It has two rectangular pieces of copper within it and a cone shape hole extending through it. A sphere of air extending 20 cm in radius from the origin surrounds the cube. The density of this air was increased from .01g/cc to .6, .8, 1.5, 2, and 3 g/cc, which effectively increased the

track-length tally of K_{eff} (Tally 14) by 7%, 9%, 16%, 21%, and 30%, respectively.

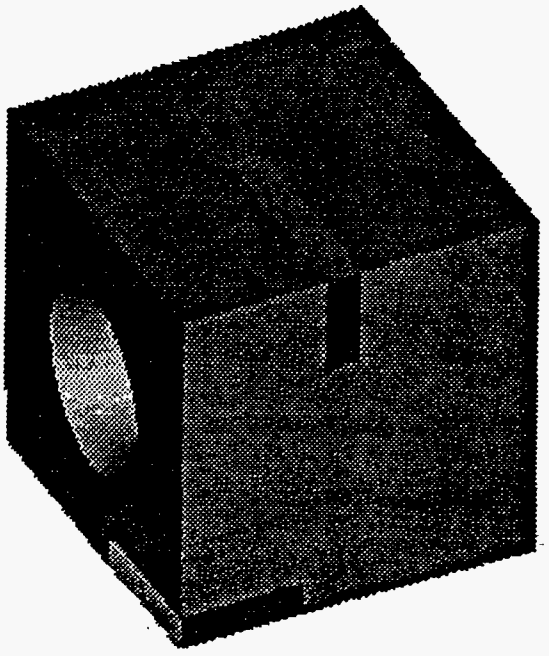

Fig. 1. A view of criticality problem INP09, showing the ^{235}U cube, copper plates, and conical hole.

Table I lists the actual and predicted percent changes to Tally 14, along with their relative errors. The actual changes were calculated by performing separate MCNP runs and correctly combining their relative errors. The predicted changes were calculated all within a single run using five appropriate PERT cards. Figure 2 plots these results and indicates the accuracy of this method (first and second order) is acceptable up to 10-15% changes in K_{eff}. The deviation from the actual changes is most likely due to changes in the shape of the eigenfunction which is currently not accounted for.

Table I. Actual and predicted values of K_{eff} for perturbations in air density of INP09.

	Air Density (g/cc)					
	.01	0.6	0.8	1.5	2.0	3.0
Actual						
K_{eff}	1.009	1.078	1.100	1.175	1.223	1.308
Rel. Error	.0001	.0015	.0017	.0021	.0022	.0025
% Change		6.81	8.94	16.41	21.14	29.56
Rel. Error		.0219	.0189	.0127	.0103	.0084
Predicted						
ΔK_{eff}		.0837	.1121	.2114	.2823	.4241
Rel. Error		.0167	.0221	.0411	.0547	.0820
% Change		8.29	11.11	20.95	27.97	42.02
Rel. Error		.0167	.0221	.0411	.0547	.0820

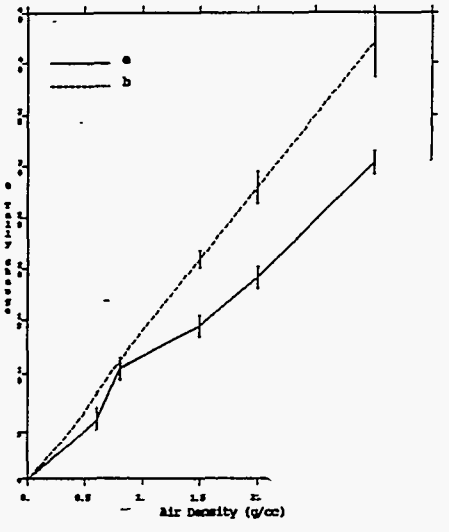

Fig. 2. Actual and predicted percent change in K_{eff} versus air density for INP09.

Second Problem

This problem is INP18 from the MCNP test set and is comprised of a hexagonal prism lattice in the shape of a cylindrical reactor (see figure 3). It is cut in half and uses a reflective plane for simplification. The fuel is 70% enriched uranium in the shape of cylindrical rods. The clad on the fuel is a mixture of zirconium and niobium with a inner liner of tungsten. Inside the clad, water blankets the fuel for cooling. Water is also used as the moderator and heat transfer agent for the reactor outside the fuel rods. There are three half control rods and five whole ones, made of ^{10}B, ^{11}B, and carbon. The control rods are encased in the same zirconium and niobium clad as the fuel, but without a liner. The sheath for the control rod is also made of zirconium and niobium and has water that traverses between the sheath and clad. The water is a mixture of heavy and light water. The water density was increased from 1 g/cc to 2, 3, 4, and 6 g/cc, which increased the track-length tally of K_{eff} (Tally 14) by 9%, 15%, 21%, and 30%, respectively.

Table II lists the actual and predicted percent changes to Tally 14, along with their relative errors. Once again, the predicted changes were calculated all within a single run using four appropriate PERT cards. Figure 4 plots this data and indicates the accuracy is quite good up to 20-25% changes in K_{eff}.

Table II. Actual and predicted values of K_{eff} for perturbations in water density of INP18.

	Water Density (g/cc)				
	1.0	**2.0**	**3.0**	**4.0**	**6.0**
Actual					
K_{eff}	1.037	1.126	1.195	1.253	1.344
Rel. Error	.0003	.0016	.0016	.0016	.0018
% Change		8.60	15.20	20.81	29.59
Rel. Error		.0183	.0103	.0075	.0060
Predicted					
ΔK_{eff}		.0954	.1669	.2144	.2376
Rel. Error		.0186	.0349	.0581	.1410
% Change		9.20	16.10	20.68	22.92
Rel. Error		.0186	.0349	.0581	.1410

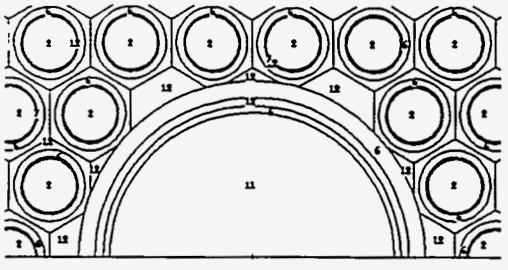

Fig. 3. A view of criticality problem INP18, showing the triangular pitched fuel rods, moderator, and control rods.

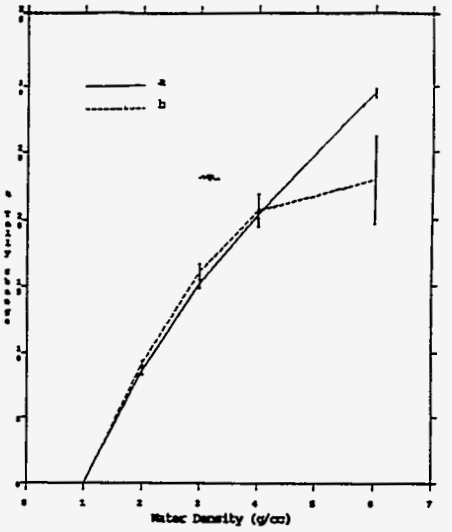

Fig. 4. Actual and predicted percent change in K_{eff} versus air density for INP18.

CONCLUSIONS

The differential operator perturbation technique implemented into future versions of MCNP will provide the radiation transport analyst with a powerful tool for estimating the effect of multiple perturbations within a single run. This technique has shown to provide adequate accuracy for up to 20-30% changes in a response for fixed-source problems and up to 10-20% changes in K_{eff} for criticality problems.

REFERENCES

1. Briesmeister, J., Editor, "MCNP - A General Monte Carlo N-Particle Transport Code," LA-12625-M, Los Alamos National Laboratory (1993).
2. Takahashi, H., "Monte Carlo Method for Geometrical Perturbation and its Application to the Pulsed Fast Reactor," Nucl. Sci. Eng. **41**, p. 259 (1970).
3. Hall, M. C., "Monte Carlo Perturbation Theory in Neutron Transport Calculations," Ph. D. Thesis, University of London (1980).
4. Hall, M. C., "Cross Section Adjustment with Monte Carlo Sensitivities: Application to the Winfrith Iron Benchmark," Nucl. Sci. Eng. **81**, p. 423 (1982).
5. Rief, H., "Generalized Monte Carlo Perturbation Algorithms for Correlated Sampling and a Second-Order Taylor Series Approach," Ann. Nucl. Energy **11**, p. 455 (1984).
6. McKinney, G., "A Monte Carlo (MCNP) Sensitivity Code Development and Application," M.S. Thesis, University of Washington (1984).
7. McKinney et. al., G., "Verification of the Monte Carlo Differential Operator Technique for MCNP," To be Published, Los Alamos National Laboratory (1995).